

POWER SYSTEM OSCILLATIONS DAMPING BY A DYNAMIC STATE ESTIMATOR CONTROL METHOD

B Vijaya Bhaskar Reddy¹, D Janardhana²

¹M.Tech, MJR college of engineering & technology, piler, chittoor dist, AP

²Asst.Prof, MJR college of engineering & technology, piler, chittoor dist, AP

Abstract: Power system oscillations damping is very important in case of inter area connected power system. This paper proposes a dynamic state estimator method (DSE) for damping oscillations with the aid of SVC type facts controller. In this paper the state of a system is accurately measured by DSE using PMU and new method. Proposed method is tested on IEEE 50 generator system, the results demonstrated that the proposed method is effectively damping the oscillations compared with existing system.

Keywords: Stability, power system damping, Kalman filter, state estimation, power system control, dynamic state estimator.

I.INTRODUCTION

The use of power system stabilizers (PSSs) has been the first measure to enhance small signal stability by damping oscillations. However, local signal based controls may not always be feasible or effective to damp inter area modes because of the lack of observability of the system modal characteristics. In such cases, remote signals are employed [1], taking into consideration the time delay in data communication [2]. This required remote signal sometimes is not available, or the signal quality can degrade the performance of damping controllers [3]. With the development and installation of PMUs in large scale electric power systems, data can be available at high sampling rates with high speed communication channels, thus opening the avenue to new monitoring and control applications [4], [5]. The typical PMU sampling rate of 10 to 120 samples per second has allowed capturing the dynamics of electromechanical oscillations in near real time. A control scheme to improve small signal based control using dynamic state estimation (DSE) and utilizing Kalman filter (KF) theory has been applied to the synchronous machine in [6]. Consequently, the local modes of a single machine infinite bus system are improved by the supplementary control of a static var compensator (SVC). The rotor speed deviation is estimated and utilized as a control signal.

In the literature, the algorithm proposed in [7] by Ghahremani and Kamwa is applied to a multi-machine system and requires the coordination of the local power system stabilizers (PSSs) with wide-area PSS controllers. This approach requires that control signals are estimated signals from remote generators. This approach is applied to the Kundur four machine test system in [8]. A decentralized LQG control scheme is proposed in [9]: the DSE method and the extended linear quadratic regulator for optimal control are applied to those controllable generators using local measurements. This algorithm is applied to a 16 machine 68 bus test system. To provide damping to the system, these methods coordinate with the automatic voltage regulator of the synchronous machine, thus the PSSs installed need to be upgraded. In some cases, the supplementary damping controls (SDCs) are already adjusted for an optimal improvement of local stability.

In a broader context, the power system oscillation problem has also been related to voltage stability [10]. In this case, the PSS system does not play a significant role as compared to FACTS devices which can increase the stability by local voltage control. The control interaction is discussed in [11]-[13].

In this paper, a different approach is taken: a control signal is obtained using an estimated signal from a DSE, and the supplementary control is implemented using a static VAR compensator embedded in the transmission network. The proposed approach is detailed in the rest of this paper, which is structured as follows: Section II conceptually explains how the damping enhancement is performed by employing an SVC and estimated supplementary control signals obtained from a DSE. The conceptual approach is mathematically formalized in Section III. Section IV briefly emphasizes the contributions of this paper. In Section V, the performance of the proposed control scheme is evaluated on the IEEE 50-generator test system through time domain simulation and small-signal analysis. Finally, concluding remarks are given in Section V.

II.PROPOSED CONTROL METHOD

To obtain wide area signals from the transmission system (e.g., the line current magnitudes), the power system model is represented by Holt's exponential smoothing technique [21] as,

$$\mathbf{x}_k = \mathbf{F}_{k-1} \mathbf{x}_{k-1} + \mathbf{g}_{k-1} + \mathbf{w}_{k-1} \quad (1)$$

where the subscripts k and $k-1$ denote two successive discrete time instants separated by T_s seconds; \mathbf{x}_k is the predicted state vector, \mathbf{x}_{k-1} is the true state vector composed of phase angles θ_{k-1} (in radians) and voltage magnitudes V_{k-1} (pu). The model error \mathbf{w}_{k-1} is represented by Gaussian noise with zero mean and covariance matrix \mathbf{Q}_{k-1} . Matrix \mathbf{F}_{k-1} and vector \mathbf{g}_{k-1} are calculated as,

$$\begin{aligned} \mathbf{F}_{k-1} &= \alpha(1 + \beta)\mathbf{I} \\ \mathbf{g}_{k-1} &= (1 + \beta)(1 - \alpha)\mathbf{x}_{k-1} - \beta\mathbf{a}_{k-2} + (1 - \beta)\mathbf{b}_{k-2} \\ \mathbf{a}_{k-1} &= \alpha\mathbf{x}_{k-1} + (1 - \alpha)\mathbf{x}_{k-1} \\ \mathbf{b}_{k-1} &= \beta(\mathbf{a}_{k-1} - \mathbf{a}_{k-2}) + (1 - \beta)\mathbf{b}_{k-2} \end{aligned} \quad (2)$$

where \mathbf{I} is the identity matrix; α and β are the parameters lying in the range from 0 to 1. In this formulation, bold face denotes vectors and matrices. The measurement model is given by,

$$\mathbf{z}_k = \mathbf{h}_k(\mathbf{x}_k) + \boldsymbol{\varsigma}_k \quad (3)$$

where \mathbf{z}_k is the measurement vector related to state variables through the nonlinear functions \mathbf{h}_k . The set of measurements from PMUs include, the bus voltage phasor quantities V_{PMU} (pu) and phase angle θ_{PMU} (rad) in addition to the branch current phasor for the transmission components $I_{branch,r}$ (pu) and $I_{branch,i}$ (pu) in rectangular form. These measurements have conventional mathematical models as given in [22], [23]. The measurement error $\boldsymbol{\epsilon}_k$ is represented by Gaussian noise with zero mean and covariance matrix \mathbf{R}_k .

The noise sequences \mathbf{w}_{k-1} and $\boldsymbol{\epsilon}_k$ are considered to be white, Gaussian and independent of each other. Then the extended Kalman filter (EKF) is applied to (1) and (3). The prediction and update steps are [24] as follows:

1. Initialization of the filter at $k = 0$, the estimated state vector $\hat{\mathbf{x}}_0$ and the covariance matrix \mathbf{P}_0 are computed as

$$\begin{aligned} \hat{\mathbf{x}}_0 &= E[\mathbf{x}_0] \\ \mathbf{P}_0 &= E[(\mathbf{x}_0 - \hat{\mathbf{x}}_0)(\mathbf{x}_0 - \hat{\mathbf{x}}_0)^T] \end{aligned} \quad (4)$$

Where E indicates the expected value.

2. Prediction: the predicted state \mathbf{x}_k and predicted covariance \mathbf{P}_k are calculated as

$$\begin{aligned} \hat{\mathbf{x}}_k &= \mathbf{F}_{k-1} \hat{\mathbf{x}}_{k-1} + \mathbf{g}_{k-1} + \mathbf{w}_{k-1} \\ \mathbf{P}_k^- &= \mathbf{F}_{k-1} \mathbf{P}_{k-1} \mathbf{F}_{k-1}^T + \mathbf{Q}_{k-1} \end{aligned} \quad (5)$$

3. Update: the estimated state vector \mathbf{x}_k and the covariance matrix \mathbf{P}_k are give by

$$\begin{aligned} \hat{\mathbf{x}}_k &= \hat{\mathbf{x}}_k^- + \mathbf{K}_k [\mathbf{z}_k - \mathbf{h}_k(\hat{\mathbf{x}}_k^-)] \\ \mathbf{P}_k &= (\mathbf{I} - \mathbf{K}_k \mathbf{H}_k) \mathbf{P}_k^- \end{aligned} \quad (6)$$

where the gain \mathbf{K}_k and \mathbf{H}_k are expressed as

$$\begin{aligned} \mathbf{K}_k &= \mathbf{P}_k^- \mathbf{H}_k^T (\mathbf{H}_k \mathbf{P}_k^- \mathbf{H}_k^T + \mathbf{R}_k)^{-1} \\ \mathbf{H}_k &= \left. \frac{\partial \mathbf{h}_k}{\partial \mathbf{x}} \right|_{\hat{\mathbf{x}}_{k-1}} \end{aligned} \quad (7)$$

3. Finally, at discrete time k , the magnitude of branch current is in function of the state vector is computed as

$$I_{pq,k}^{\wedge}(\hat{\mathbf{x}}_k) = \left| \frac{V_{p,k}^{\wedge} \angle \theta_{p,k}^{\wedge} - V_{q,k}^{\wedge} \angle \theta_{q,k}^{\wedge}}{z_{pq}} \right| \quad (8)$$

Where z_{pq} is the primitive series impedance of the element between the buses p and q . References [25-26] note that the use of conventional bad data analysis can fail when applied to PMU's measurements because their errors have a non-Gaussian distribution. Hence, to identify gross errors in measurements, the EKF

algorithm can be used to define the innovation process vector and for the i th measurement the normalized innovation process [27] as

$$v_k = -h_k(x_k) + z_k$$

$$\lambda_{k,i} = \frac{v_{k,i}}{\rho_{k,i}}, i = 1, 2, \dots, m \quad (9)$$

Where

$$\rho_{k,i}^2 = H_{k,i} P_{k,i}^- H_{k,i}^T + \sigma_i^2 \quad (10)$$

in which $H_{k,i}$ is the i th row of H_k and V_i^2 is the i th diagonal element of R_k . In this paper, the criterion for bad data detection is defined by

$$|\lambda_{k,i}| > \lambda_{\max}, i = 1, 2, \dots, m \quad (11)$$

where the threshold value λ_{\max} is system dependent and determined using offline simulations. The measurement value with bad data is replaced by the predicted value.

The power system model in (1) has been reported in [21], [28], [29] by assuming a quasi-steady state behavior of the system and monitored in a time steps of a few minutes. Taking these facts into account, a $T_s = 10$ ms is considered in this paper. With a significant variation in the system resulting from a large disturbance, the performance of the DSE could be affected due to the value of the state prediction in (5) which is based on the values of state at the time previous to the disturbance. To handle this issue, bad data detection is utilized. A large disturbance is detected in the above EKF algorithm when those measurements of voltage magnitude V_{PMU} at different buses of the network are identified with gross error simultaneously in (10). In this case, the bad data detection is not considered, and the values of the covariance matrix Q related to the bad measurements are modified instead of replacing the bad data by predicted values. This means that the model prediction is not weighted in the estimation process during large variations in the power system.

NEW CONTROL SCHEME FOR INTER AREA OSCILLATIONS:

The main advantages of the proposed power system damping controllers are:

- The proposed supplementary damping controller for the large power system is implemented in an SVC and derives the wide area control input using the estimator. The availability and quality of the wide area control signal or stabilizing signal are ensured by using the DSE method
- The controller does not require any change in the PSS setting at the synchronous machine.
- An alternative control signal can be obtained. This function is useful when the system is not observable, and the required control signal cannot be estimated due to the PMUs configuration.
- Communication failures and transmissions delay for the stabilizing signal from the estimator are considered in the robust controller.

As shown in Fig. 1, a, b, c are three nodes. Z_1 and Z_2 are the impedance of line 1 and line 2 respectively. S_1' and S_1'' are the power of the start and the end of line 1 respectively. S_2' and S_2'' the power at the start and end of line 2 respectively. S_b and S_c is the load of node b and node c respectively.

In the power system without PV generation, some equations can be obtained according to the simple power flow calculation method.

The power at the end of line 2 is

$$S_2' = S_c \quad (1)$$

The power loss of line 2 is

$$\Delta S_2 = \left(\frac{S_2'}{V_N} \right)^2 \times (R_2 + jX_2) \quad (2)$$

The power at the start of line 2 is written as:

$$S_2' = S'' + \Delta S_2 \quad (3)$$

The power at the end of the line 1 is

$$S_2' = S_b + S_2' \quad (4)$$

The power loss of the line 1 is

$$\Delta S_1 = \left(\frac{S'_1}{V_N} \right)^2 \times (R_1 + jX_1) \quad (5)$$

The power at the start of line 2 is written as:

$$S'_1 = S''_1 + \Delta S_1 \quad (6)$$

The loss of voltage longitudinal component of line 1 is

$$\Delta V_1 = \left(\frac{P'_1 R_1 + Q'_1 X_1}{V_N} \right) \quad (7)$$

$$V_b = V_a - \Delta V_1 \quad (8)$$

The loss of voltage longitudinal component of line 1 is

$$\Delta V_2 = \left(\frac{P'_2 R_2 + Q'_2 X_2}{V_N} \right) \quad (9)$$

$$V_c = V_b - \Delta V_2 \quad (10)$$

It is assumed that the voltages of node b, c have meet the error requirements. It is obviously that the voltage of node c is smaller than b, b is smaller than a. When adding the PV station on node c, in order to clarify the problem more clearly, we assume that the reactive power of the PV plant Q_{PV} and Q_c are both zero, active power P_{PV} is larger than P_c . We can see that PV plant is not only to meet the load demand of node c, but also provide power to the grid. S_2'' and S_20 are negative and have the opposite direction with original direction without PV. $S_1\}$ and S_10 become smaller than before. Therefore, V_1 becomes smaller and V_b becomes larger, V_2 becomes negative. The volt-age of node c is larger than node b. From the above analysis, we can see that the voltage of node c is larger than node b after the access of PV plant. This is only a simple three-node system analysis. In fact, the number of network nodes and PV plants are more so that the situation of voltage is more complicated. The traditional way of voltage regulation, for example, the on-load tap changer, may lead to make a node to return to normal, while the other nodes are beyond the allow-able range. With the increasing configuration of DESSs on PV plants, the use of DESS for voltage regulation becomes a new regulated method. DESS can regulates voltage by a variety of ways, such as absorption or generation of active power, absorption or generation of reactive power, combination of active power and reactive power [15– 17].

III . TEST SYSTEM & RESULTS

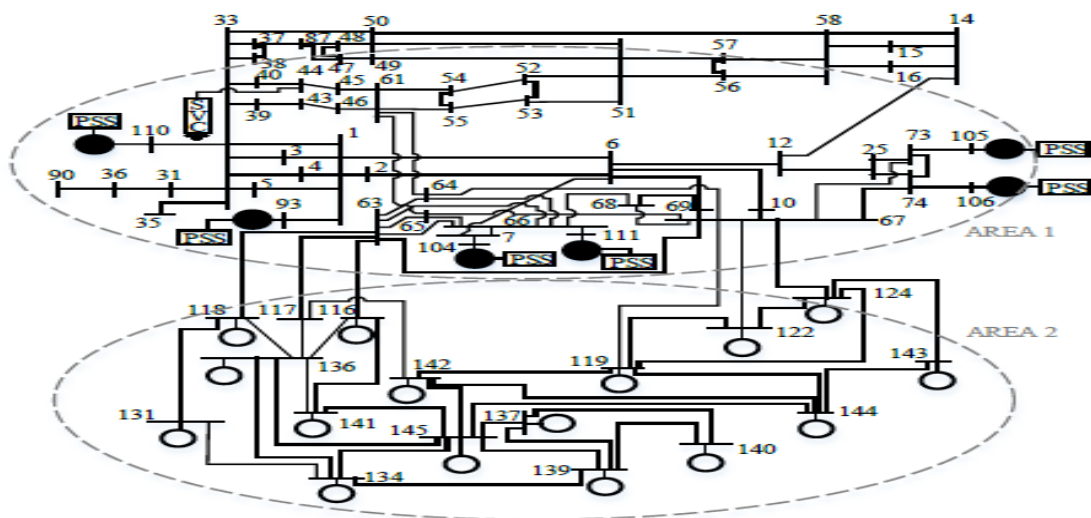


Fig. 1. One-line diagram of the IEEE 50-generator system with areas of interest encircled [35].

A. Robustness at nominal operating condition

The proposed method is applied to the IEEE 50-generator system [30]. The robust SDC associated with the SVC reported in [17] is considered: this FACTS device is optimally located at bus #44 and its rating is $Q_C = Q_L = \pm 400$ MVar. The SDC limiter bounds are set at $V_{sup_max} = 0.1$ and $V_{sup_min} = -0.1$ pu, and the nominal transmission delay is considered to be 100ms. The impact of latency of measurements and missing data are discussed in [31]-[32]. This moderate sized system with 145 buses has all the modeling features and complexity of a large scale power system. The one-line diagram of the system with areas of interest is shown in Fig. 3. Six generators are represented by the 2 axis model with the IEEE AC-4 excitation system and PSS, 44 generators are represented by the classical model. All loads are assumed to be constant impedance. The dynamic parameters of the system are available in [33] For the purpose of this paper, the PMUs are located for ensuring system's observability and the study reported in [17] is used to determine the suitable location of the SVC for damping out power oscillations.

Study of this system shows that the system has a critical inter area mode near 0.28 Hz and the system stability limit is identified by adjusting the active power of generators #93 and #110. The SDC control signal actuates the SVC and the damping provided by the PSS is improved. These statements are supported by the eigen analysis applied to the test system with program SSAT [34], the results are shown in Table I. The SDC utilized in this example requires a current magnitude on line 63-66 and line 44-45 for the wide-area control input and local control input z respectively. These signals are identified as the best candidate by the criteria of residues and observability factor [1] for the design of the controller.

The results of damping control for the cases A, B and C are illustrated in Figs. 2 and 3.

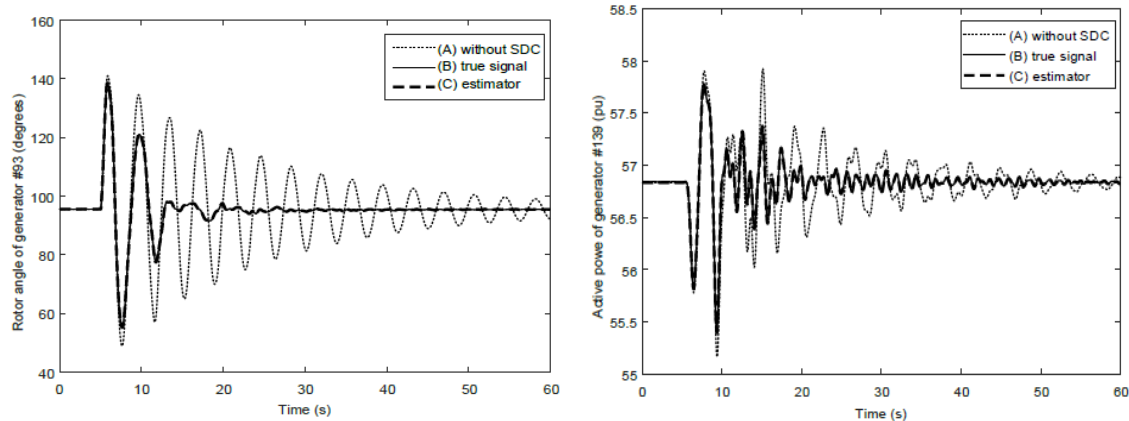


Fig. 2 & 3. Response of rotor angle of generator at #93 & #139 (Area 1) to the large disturbance (2×1700 MW) for the cases A, B and C.

The DSE provides the wide-area signal required by the controller as shown in Fig. 4, the estimated current line magnitude on line 63-66 is similar to the true signal; however, there is a small difference for a few milliseconds after the fault is cleared; this error in the estimated signal does not significantly impact the response of the SDC. The dynamics of monitored variable in case A reflects the lack of damping control provided by the SVC alone. Fig. 5 shows the output of the supplementary controller of the SVC and reflects the control effort during the disturbance.

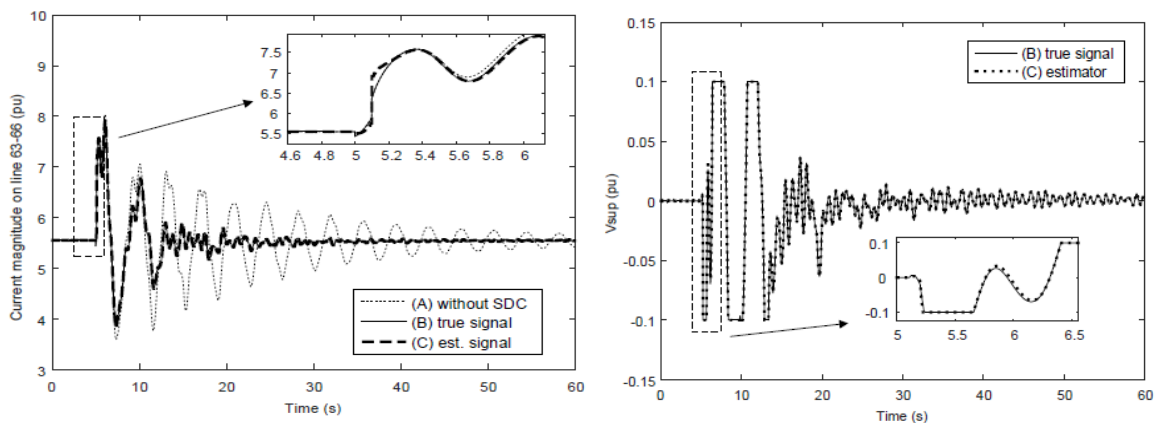


Fig. 4 & 5 Response of control & output signals required $|I_{63-66}|$ by the SDC to large disturbance (2×1700 MW) for the cases A and C.

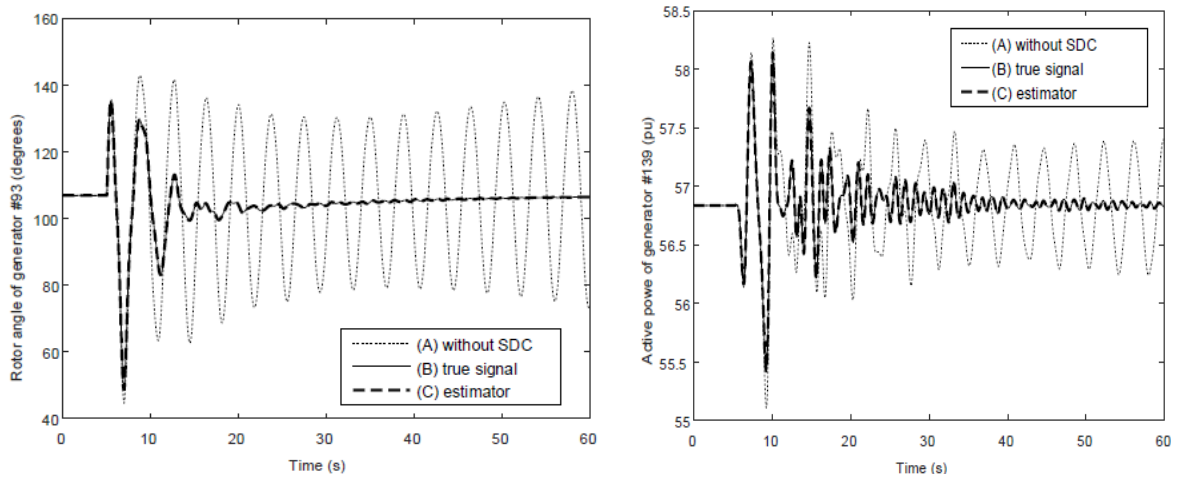


Fig. 6&7. Response of active power of generator at #93 and #139 (Area 2) to large disturbance (2×1800 MW) for the cases A, B and C.

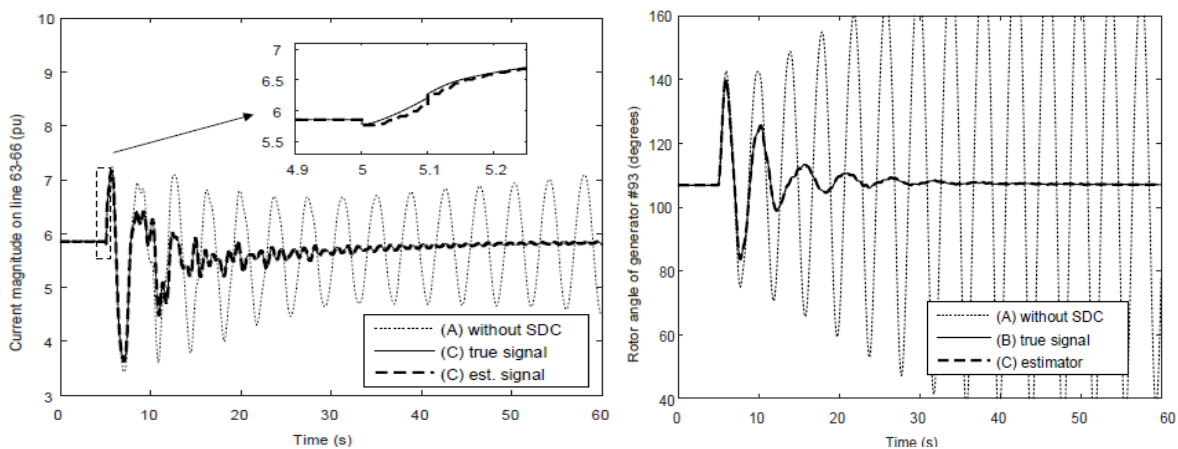


Fig. 8 & 9. Response of control signal required $|I_{63-66}|$ by the SDC and rotor angle oscillations to disturbance (2×1800 MW) for the cases A and C.

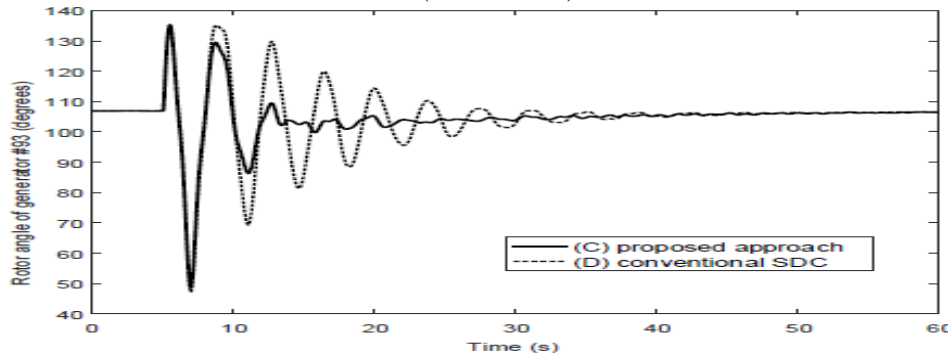


Fig. 11. Response of rotor angle of generator #93 (Area 1) to large disturbance (2×1800 MW) for the cases C and D.

B. Robustness to different operating conditions

The response of the system to the large disturbance for the cases A, B and C is illustrated in Figs. 6 and 7. As shown in Fig. 8, the estimated control signal follows the actual signal in case C quite closely to the response of the system during the event except during the fault. The oscillations associated with the rotor angle of generator #93 are shown in Figs. 9 and 10 for each scenario, respectively.

IV . CONCLUSIONS

An alternative control scheme for damping of electromechanical oscillations in a multi-machine system by means of an SVC and the use of the DSE method to obtain a stabilizing signal has been presented. PMU measurements and transmission system parameters are employed in the estimator to provide the required wide area signal to the robust supplementary controller for the SVC. The IEEE 50

test system was used to illustrate the method. Small signal analysis was conducted to evaluate the interaction between SDC in a large scale power system. Results for the rotor angle and the active power of those generators with large participation in the critical mode show satisfactory performance of the proposed method by improving the damping control afforded by the PSSs. The estimator provided a control signal accurately as confirmed by the response of the supplementary controller. This conformation is observed in comparison to control when a true signal is utilized. Furthermore, the proposed method demonstrates the use of an alternative wide area signal for the SDC. Measurements at different noise levels, variations of the system operating conditions, as well different locations of fault were assessed.

REFERENCES:

- [1] J. Chow, J. Sánchez-Gasca, H. Ren, S. Wang, "Power system damping controller design using multiple input signals," *IEEE Control Systems Magazine*, vol. 20, no. 4, pp. 82-90, Aug. 2000.
- [2] H. Wu, K. S. Tsakalis, and G. T. Heydt, "Evaluation of time delay effects to wide-area power system stabilizer design," *IEEE Trans. Power Syst.*, vol. 19, no. 4, pp. 1935–1941, Nov. 2004.
- [3] M. S. Almas and L. Vanfretti, "Impact of time-synchronization signal loss on PMU-based WAMPAC applications," *Proc. IEEE Power Engineering Society General Meeting*, Boston, 2016.
- [4] H. Li, A. Bose, V. Venkatasubramanian, "Wide-area voltage monitoring and optimization," *IEEE Transactions on Smart Grid*, vol. 7, no. 2, pp. 785–793, March 2016.
- [5] A. G. Phadke and J. S. Thorp, *Synchronized Phasor Measurements and their Application*. New York: Springer, 2008.
- [6] I. L. Ortega Rivera, C. R. Fuerte Esquivel, C. Angeles Camacho, G. T. Heydt, V. Vittal, "A dynamic state estimator for the development of a Control Signal for Power System Damping Enhancement," *Proc. IEEE Innovative Smart Grid Technologies (IGST)*, Arlington, VA, April, 2017.
- [7] E. Ghahremani, I. Kamwa, "Local and wide-area PMU-based decentralized dynamic state estimation in multi-machine power systems," *IEEE Transactions on Power Systems*, vol. 31, no. 1, pp. 547–562, 2016.
- [8] P. Kundur, *Power system stability and control*, McGraw Hill Book Co., New York, NY, 1994.
- [9] A. K. Singh and B. C. Pal, "Decentralized control of oscillatory dynamics in power systems using an extended LQR," *IEEE Trans. Power Syst.*, vol. 31, no. 3, pp. 1715–1728, May 2016.
- [10] N. Mithulananthan, C. A. Cañizares, and J. Reeve, "Hopf bifurcation control in power system using power system stabilizers and static var compensator," in *Proc. North American Power Symposium*, San Luis Obispo, CA, Oct. 1999, pp. 155 – 163.
- [11] N. Mithulananthan, C. A. Cañizares, J. Reeve, G. J. Rogers, "Comparison of PSS, SVC, and STATCOM controllers for damping power system oscillations," *IEEE Transactions on Power Systems*, vol. 18, no. 2, pp. 786 – 792, 2003.
- [12] H. K. Tyll, F. Schettler, "Power system problems solved by FACTS devices," *Proc. IEEE Power Systems Conference and Exposition*, pp. 1 – 5, 2009.
- [13] X. Y. Bian, Y. Gen, K. L. Lo, Y. Fu, Q. B. Zhou, "Coordination of PSSs and SVC damping controller to improve probabilistic small-signal stability of power system with wind farm integration," *IEEE Trans. Power Syst.*, vol. 31, no. 3, pp. 2371–2382, May 2016.
- [14] T. Ohyama; K. Yamashita, T. Maeda, H. Suzuki; S. Mine, "Effective application of static var compensators to damp oscillations," *IEEE Transactions on Power Apparatus and Systems*, vol. PAS-104, no. 6, pp. 1405 – 1410, 1985.
- [15] E. V. Larsen and L. H. Chow, "SVC control design concepts for system dynamic performance," in *IEEE Tutorial Course: Application of SVS for System Dynamic Performance*, 1987, pp. 36–53, 87TH0187-5-PWR.
- [16] R. E. Kalman, "A new approach to linear filtering and prediction problems," *ASME J. Basic Eng.*, vol. 82, pp. 35–45, 1960.
- [17] S. Zhang and V. Vittal, "Design of wide-area power system damping controllers resilient to communication failures," *IEEE Trans. Power Syst.*, vol. 28, no. 4, pp. 4292–4300, Nov. 2013.
- [18] A. G. Phadke and B. Kasztenny, "Synchronized phasor and frequency measurement under transient conditions," *IEEE Trans. Power Delivery*, vol. 24, no. 1, pp. 89–95, Jan. 2009.
- [19] P. Zarco and A. G. Expósito, "Power system parameter estimation: A survey," *IEEE Trans. Power Syst.*, vol. 15, no. 1, pp. 216–222, Feb. 2000.
- [20] S. A. Arafteh and R. Schinzinger, "Estimation algorithms for large-scale power systems," *IEEE Trans. Power App. Syst.*, vol. PAS-98, no. 6, pp. 1968–1977, Nov. 1979.
- [21] A. M. Leite da Silva, M. B. Do Coutto Filho, and J. F. de Queiroz, "State forecasting in electric power systems," *Proc. IEE on Gener. Trans. Distrib.*, vol. 130, no. 5, pp. 237–244, Sept. 1983.

- [22] A. Abur and A. G. Expósito, Power system state estimation: theory and implementation. New York: Marcel Dekker, 2004.
- [23] E. A. Zamora-Cárdenas, B. A. Alcaide-Moreno, C.R. Fuerte-Esquivel, "State estimation of flexible AC transmission systems considering synchronized phasor measurements," Electric Power Systems Research, vol. 106, pp. 120–133, 2014.
- [24] D. Simon, Optimal State Estimation; Kalman, H_∞ and Nonlinear Approaches. Hoboken, NJ: Wiley, 2006.
- [25] L. Zhang and A. Abur, "Impact of tuning on bad data detection of PMU measurements," in Proc. IEEE Innovative Smart Grid TechnologiesAsia, Tianjin, China, May 2012, pp. 1-5.
- [26] S. Wang, J. Zhao, Z. Huang and R. Diao, "Assessing Gaussian Assumption of PMU Measurement Error Using Field Data," IEEE Trans. on Power Delivery, vol. PP, IEEE early access articles, pp. 1-3, 2017,
- [27] K. Nishiya, J. Hasegawa, and T. Koike, "Dynamic state estimation including anomaly detection and identification for power systems," IEE Proceedings on Generation, Transmission and Distribution, vol. 129, no. 5, pp. 192-198, 1982.
- [28] P. Rousseaux, T. Van Cutsem, T. E. Dy Liacco, "Whither dynamic state estimation?" Int. J. Elect. Power Energy Syst., vol. 12, no. 2, pp. 104–116, Apr. 1990.
- [29] G. Valverde, V. Terzija, "Unscented Kalman filter for power system dynamic state estimation", IET Gener. Transm. Distrib., vol. 5, no. 1, pp. 29-37, Jan. 2011.
- [30] V. Vittal, Chair, "Transient stability test systems for direct stability methods," IEEE Trans Power Syst., vol. 7, no. 1, pp. 37–43, Feb. 1992.
- [31] B. Naduvathuparambil, M. C. Valenti, and A. Feliachi, "Communication delays in wide area measurement systems," in Proc. 34th Southeastern Symp. Syst. Theory, Huntsville, AL, USA, Mar. 2002, pp. 118–122.
- [32] B.A. Alcaide-Moreno, C.R. Fuerte-Esquivel, M. Glavic and T. Van Cutsem, "Electric power network state tracking from multirate measurements," IEEE Trans. Instrum. Meas., vol. 67, no. 1, pp. 33–44, January 2018.
- [33] S. Zhang, "Improved power grid resiliency through interactive system control," Ph.D. dissertation, Arizona State Univ., Tempe, AZ., 2014.
- [34] Powertech, Small Signal Analysis Tool (SSAT) User Manual, Powertech Labs. Surrey, BC, Canada, 2015.
- [35] S. Zhang, V. Vittal, "Wide-area control resiliency using redundant communication paths," IEEE Trans. on Power Systems, vol. 29, no. 5, pp. 2189–2199, September, 2014.
- [36] Powertech, Transient Stability Analysis Tool (TSAT) User Manual, Powertech Labs. Surrey, BC, Canada, 2015.
- [37] Powertech, User-defined Model Manual for Transient Security Assessment Tool, Powertech Labs. Surrey, BC, Canada, 2015. luation of distribution system including wind/solar dg.